

Fermionic Partial Transpose in the Overlap Matrix Framework for Entanglement Negativity

Jun Qi Fang¹ and Xiao Yan Xu^{1,2,*}

¹Key Laboratory of Artificial Structures and Quantum Control (Ministry of Education),
School of Physics and Astronomy, Shanghai Jiao Tong University, Shanghai 200240, China

²Hefei National Laboratory, Hefei 230088, China

(Dated: March 13, 2025)

Over the past two decades, the overlap matrix approach has been developed to compute quantum entanglement in free-fermion systems, particularly to calculate entanglement entropy and entanglement negativity. This method involves the use of partial trace and partial transpose operations within the overlap matrix framework. However, previous studies have only considered the conventional partial transpose in fermionic systems, which does not account for fermionic anticommutation relations. Although the concept of a fermionic partial transpose was introduced in [1], it has not yet been systematically incorporated into the overlap matrix framework. In this paper, we introduce the fermionic partial transpose into the overlap matrix approach, provide a systematic analysis of the validity of partial trace and partial transpose operations, and derive an explicit formula for calculating entanglement negativity in bipartite systems. Additionally, we numerically compute the logarithmic negativity of two lattice models to verify the Goev-Klich-Widom scaling law. For tripartite geometries, we uncover limitations of the overlap matrix method and demonstrate that the previously reported logarithmic negativity result for a homogeneous one-dimensional chain in a disjoint interval geometry exceeds its theoretical upper bound. Our findings contribute to a deeper understanding of partial trace and partial transpose operations in different representations.

I. INTRODUCTION

Research on quantum entanglement in recent decades has offered a novel perspective on the analysis of many-body states in condensed matter physics [2–5]. Unlike classical correlations, quantum entanglement reveals the intrinsic connections between subsystems of a quantum state. This unique property has made quantum entanglement a critical framework for understanding collective behaviors, quantum phase transitions, topological order, and quantum criticality in condensed matter systems [6–10]. Among the various measures of entanglement, the entanglement entropy has proven to be particularly effective in characterizing bipartite entanglement in the ground states of many-body systems [5, 11, 12].

However, for mixed states, such as tripartite systems and thermal states, entanglement entropy alone cannot fully characterize entanglement, as it also includes contributions from classical correlations. To address this limitation, several measures have been proposed to quantify entanglement in mixed states [13]. Among these, entanglement negativity [14–16], based on the partial transpose operation, is widely used. One of the key features of this measure is that, for separable states, the eigenvalues of the density matrix remain non-negative after applying the partial transpose operation [17, 18], making it a powerful diagnostic tool for identifying entanglement.

Compared to other mixed state entanglement measures, entanglement negativity has the advantage of requiring only straightforward linear algebra computations. In this paper, we focus on logarithmic negativity, which is defined as follows. Given the density matrix of a mixed state, such as a reduced density matrix obtained by tracing out region B while retain-

ing $\rho_{A_1 \cup A_2}$, the logarithmic negativity is given by

$$\mathcal{E} = \ln \text{Tr} \left| \rho_{A_1 \cup A_2}^{T_{A_2}} \right|, \quad (1)$$

where $\rho_{A_1 \cup A_2}^{T_{A_2}}$ denotes the partial transpose operation on region A_2 over the reduced density matrix $\rho_{A_1 \cup A_2}$, and the trace norm operation $\text{Tr} |O|$ represents the sum of the square roots of the eigenvalues of $O^\dagger O$. If O is Hermitian, the trace norm simplifies to the sum of the absolute eigenvalues of O , though this is not always the case. Logarithmic negativity has been extensively applied to investigate entanglement in various many-body systems, including one-dimensional harmonic oscillators [19–22], spin systems [23–30], topologically ordered phases [10, 31–33], and conformal field theory (CFT) [34–37].

The negativity depends on the definition of partial transpose. In the literature, three distinct forms of partial transposition have been studied: the bosonic partial transpose (bPT), as discussed in Ref. [38, 39]; the untwisted partial transpose (uPT), introduced in Ref. [1, 40–42]; and the twisted partial transpose (tPT), presented in Ref. [43]. In fermionic systems, the definition of partial transpose must respect the fermionic anticommuting relations. Both uPT and tPT satisfy this requirement, whereas bPT does not. Compared to bPT, uPT and tPT have advantageous properties. For example, it has been shown that a fermionic Gaussian state remains Gaussian after applying uPT or tPT [1, 40, 41, 43], making them convenient for simulating Rényi negativity using the quantum Monte Carlo (QMC) algorithm [42, 44]. Interestingly, the logarithmic negativity calculated using tPT coincides with that of uPT. Therefore, in this work, we focus solely on uPT and omit further discussion of tPT.

However, in practice, the calculation of logarithmic negativity is very challenging, even for free fermion systems. For example, the Green function approach [1, 38, 39, 43] for free-fermion systems is very powerful, but it is still difficult to ex-

* xiaoyanxu@sjtu.edu.cn

tract analytical properties of logarithmic negativity. In contrast, the overlap matrix approach has emerged as a more effective tool for computing entanglement entropy and entanglement negativity in free-fermion systems [45–49]. However, in previous applications of the overlap matrix approach, only bPT was considered. In this paper, we incorporate uPT into the overlap matrix approach. We provide a systematic proof of the validity of the uPT operation, a numerical and analytical confirmation of the partial trace operation in the bipartite geometry of free-fermion systems, and propose analytical results consistent with the CFT method. In the tripartite case, we demonstrate that the previous overlap matrix approach for computing logarithmic negativity exceeds its theoretical upper bound.

This paper is organized as follows. In Sec. II, we introduce the fermionic partial transpose in the overlap matrix approach for entanglement negativity calculation in free fermions system. In Sec. III, we establish the validity of the formula for computing entanglement negativity in bipartite pure states and prove that the partial transpose density matrix in the overlap matrix approach is related to that in Fock space through a similarity transformation. We also calculate two examples, and our numerical results are consistent with the Goev-Klich-Widom scaling law. In Sec. IV, we study the logarithmic negativity of free fermions in tripartite case, and demonstrate that in mixed states, the equivalence of partial transposition in the overlap matrix approach and in Fock space no longer holds. Consequently, we show that previously reported results for tripartite geometries violate their theoretical upper bound. Finally, in Sec. V, we summarize our findings.

II. OVERLAP MATRIX APPROACH IN FREE-FERMION SYSTEMS

We begin with a brief review of the original overlap matrix approach and introduce the fermionic partial transpose operation for entanglement negativity calculation. Consider a general Hermitian Hamiltonian of a free-fermion system

$$H = \sum_{i,j} h_{i,j} c_i^\dagger c_j = \sum_{\alpha=1}^N \epsilon_\alpha f_\alpha^\dagger f_\alpha, \quad (2)$$

where the Hermitian matrix h can be diagonalized by a unitary matrix U , such that $f_\alpha^\dagger = (c^\dagger U)_\alpha = \sum_{i=1}^N c_i^\dagger U_{i,\alpha}$ is the fermionic operator in the diagonal basis with energy ϵ_α , satisfying the anticommutation relation $\{f_\alpha, f_\beta^\dagger\} = \delta_{\alpha,\beta}$. Here, N denotes the number of lattice sites. An M -particle ground state can be written as

$$|\Psi\rangle = \prod_{\alpha=1}^M f_\alpha^\dagger |0\rangle, \quad (3)$$

where M lowest energy single particle states are occupied. We consider a bipartite system in which the lattice sites are divided into two regions, labelled by A and B . A projection operator $\mathcal{P}_{A(B)}$ can be defined to only keep the particles in $A(B)$ for a given state. Specifically, the projection

of f_α^\dagger operator satisfies $\mathcal{P}_A f_\alpha^\dagger = \sum_{i \in A} c_i^\dagger U_{i,\alpha}$ and $\mathcal{P}_B f_\alpha^\dagger = \sum_{i \in B} c_i^\dagger U_{i,\alpha}$. As expected, the sum of the projections satisfies $\mathcal{P}_A f_\alpha^\dagger + \mathcal{P}_B f_\alpha^\dagger = f_\alpha^\dagger$, ensuring completeness. An overlap matrix is then introduced

$$\begin{aligned} [M_A]_{\alpha,\beta} &= \langle \mathcal{P}_A u_\alpha | \mathcal{P}_A u_\beta \rangle \\ &= \sum_{i \in A} U_{i\alpha}^* U_{i\beta}, \quad 1 \leq \alpha, \beta \leq M \end{aligned} \quad (4)$$

where $|u_\alpha\rangle = f_\alpha^\dagger |0\rangle$ is a single-particle state. It can be easily verified that $M_{A(B)}$ is Hermitian and $M_A + M_B = 1$. Consequently, the two overlap matrices M_A and M_B can be simultaneously diagonalized as $U^\dagger M_A U = \text{diag}(\{P_\gamma\}_{\gamma=1}^M)$ and $U^\dagger M_B U = \text{diag}(\{1 - P_\gamma\}_{\gamma=1}^M)$. The eigenvalues P_γ are restricted to the range $[0, 1]$ (see Appendix A for a proof). We can use U to define a new basis

$$d_\gamma^\dagger = \sum_{\alpha=1}^M f_\alpha^\dagger U_{\alpha,\gamma}. \quad (5)$$

In this new basis, the former M -particle ground state becomes

$$|\Psi\rangle = e^{i\theta} \prod_{\gamma=1}^M d_\gamma^\dagger |0\rangle, \quad (6)$$

where the phase factor $e^{i\theta} = \det(U^\dagger)$. Another interesting property of this new basis is that the region A and B part operators separate,

$$d_\gamma^\dagger \equiv \sqrt{P_\gamma} d_{A\gamma}^\dagger + \sqrt{1 - P_\gamma} d_{B\gamma}^\dagger \quad (7)$$

where

$$d_{A\gamma}^\dagger = \frac{\sum_\alpha U_{\alpha\gamma} \mathcal{P}_A f_\alpha^\dagger}{\sqrt{P_\gamma}}, \quad d_{B\gamma}^\dagger = \frac{\sum_\alpha U_{\alpha\gamma} \mathcal{P}_B f_\alpha^\dagger}{\sqrt{1 - P_\gamma}}, \quad (8)$$

and they preserve the anticommutation relations $\{d_{A(B)\gamma}, d_{A(B)\gamma'}^\dagger\} = \delta_{\gamma\gamma'}$ and $\{d_{A(B)\gamma}^\dagger, d_{B(A)\gamma'}^\dagger\} = 0$.

Since each term in the product of Eq. (6) is independent, it follows that the system can be described as a tensor product, and consequently, the density matrix also factorizes accordingly

$$\rho = \bigotimes_{\gamma=1}^M \left[\frac{1 - P_\gamma}{\sqrt{P_\gamma(1 - P_\gamma)}} \sqrt{P_\gamma(1 - P_\gamma)} \right] \equiv \bigotimes_{\gamma=1}^M \rho_\gamma, \quad (9)$$

where the basis is ordered as $\{|0_{A\gamma} 1_{B\gamma}\rangle, |1_{A\gamma} 0_{B\gamma}\rangle\}$ and the creation operator acts as $d_{A(B)\gamma}^\dagger |0\rangle = |1_{A(B)\gamma}\rangle$. Notably, the original density matrix, which initially has dimensions $2^N \times 2^N$, is effectively reduced to $2^M \times 2^M$. This reduction occurs because other rays in the Hilbert space do not contribute to $|\Psi\rangle$, and all other matrix elements in ρ are strictly zero. It is particularly worth mentioning that the most time-consuming computation in the overlap matrix approach is the diagonalization of the $M \times M$ overlap matrix, whereas in the

Green's function approach, the most time-consuming computation is the diagonalization of the $N \times N$ Green's function matrix. Therefore, in general, the overlap matrix approach is more advantageous, as M is smaller than N .

The partial trace in d^\dagger representation yields

$$\begin{aligned} \rho_A &= \bigotimes_{\gamma=1}^M \begin{bmatrix} 1 - P_\gamma & \\ & P_\gamma \end{bmatrix} \\ &= \bigotimes_{\gamma=1}^M \rho_{A\gamma}, \end{aligned} \quad (10)$$

where the basis is ordered as $\{|0_{A\gamma}\rangle, |1_{A\gamma}\rangle\}$. Before performing the partial transposition, it is useful to outline some key properties of the uPT, as discussed in Ref. [41]. The definition in Fock space is given by

$$\begin{aligned} &(|\{n_j\}_A, \{n_j\}_B\rangle \langle \{\bar{n}_j\}_A, \{\bar{n}_j\}_B|)^{T_B^f} \\ &= (-1)^{\phi(\{n_j\}, \{\bar{n}_j\})} |\{n_j\}_A, \{n_j\}_B\rangle \langle \{\bar{n}_j\}_A, \{\bar{n}_j\}_B|, \end{aligned} \quad (11)$$

where the phase factor

$$\phi(\{n_j\}, \{\bar{n}_j\}) = \frac{[(\tau_B + \bar{\tau}_B) \bmod 2]}{2} + (\tau_A + \bar{\tau}_A)(\tau_B + \bar{\tau}_B), \quad (12)$$

where $\tau_{A(B)} = \sum_{j \in A(B)} n_j$ and $\bar{\tau}_{A(B)} = \sum_{j \in A(B)} \bar{n}_j$. This uPT: (1) preserves the tensor product structure of fermionic density matrices, whereas the bPT does not

$$(\rho_{AB} \otimes \rho'_{AB})^{T_A^f} = \rho_{AB}^{T_A^f} \otimes (\rho'_{AB})^{T_A^f}; \quad (13)$$

(2) leaves the logarithmic negativity invariant under a unitary transformation

$$\mathcal{E}(\rho) = \mathcal{E}\left[(U_A \otimes U_B) \rho (U_A^\dagger \otimes U_B^\dagger)\right]; \quad (14)$$

(3) satisfies the additivity property

$$\mathcal{E}(\rho_{AB} \otimes \rho'_{AB}) = \mathcal{E}(\rho_{AB}) + \mathcal{E}(\rho'_{AB}). \quad (15)$$

Utilizing these three essential properties, we demonstrate that the bPT for the density matrix in Ref. [47] is not appropriate, as it violates property (1) above if bPT is applied to fermionic systems [41]. To address this issue, we introduce the uPT to evaluate entanglement negativity. The uPT density matrix can be expressed as

$$\rho_{\gamma}^{T_B^f} = \bigotimes_{\gamma=1}^M \rho_{\gamma}^{T_B^f}, \quad (16)$$

with

$$\rho_{\gamma}^{T_B^f} = \begin{bmatrix} 1 - P_\gamma & & & \\ & P_\gamma & & \\ & & -i\sqrt{P_\gamma(1-P_\gamma)} & \\ & & & -i\sqrt{P_\gamma(1-P_\gamma)} \end{bmatrix}. \quad (17)$$

where the basis is ordered as $\{|0_{Ai}1_{Bi}\rangle, |1_{Ai}0_{Bi}\rangle, |0_{Ai}0_{Bi}\rangle, |1_{Ai}1_{Bi}\rangle\}$. The correctness of Eq. (10) and Eq. (17) will be discussed in detail later.

Due to the tensor product structure of the density matrix, both the entanglement entropy and entanglement negativity can be computed efficiently. As an example, consider the logarithmic negativity. The eigenvalues of the Kronecker product of two matrices, $A \otimes B$, are given by all possible products $\lambda_\mu \mu_\nu$, where λ_μ and μ_ν are the eigenvalues of A and B , respectively. For the non-Hermitian $\rho^{T_B^f}$, we need to compute the eigenvalues of $\sqrt{(\rho^{T_B^f})^\dagger \rho^{T_B^f}}$, which are given by $\{\Xi_{\gamma,\alpha}\} = \{1 - P_\gamma, P_\gamma, \sqrt{P_\gamma(1-P_\gamma)}, \sqrt{P_\gamma(1-P_\gamma)}\}$. Thus, the logarithmic negativity can be formulated as

$$\begin{aligned} \mathcal{E} &= \ln \text{Tr} |\rho^{T_B^f}| = \ln \prod_{\gamma} \sum_{\alpha} \Xi_{\gamma,\alpha} \\ &= \sum_{\gamma} \ln \left[1 + 2\sqrt{P_\gamma(1-P_\gamma)} \right]. \end{aligned} \quad (18)$$

Importantly, it is shown that this formula is identical to that of Ref. [47], even though they treated the fermionic system as a bosonic system. In contrast, our approach uses the appropriate uPT for fermionic systems, ensuring consistency with the underlying fermionic structure. The formula for Von Neumann and Rényi entropy, consistent with Ref. [45, 46], can be derived similarly, as can the Rényi negativity.

III. LOGARITHMIC NEGATIVITY OF FREE FERMIONS SYSTEM IN BIPARTITE CASE

A. Validity of partial transpose in overlap matrix approach

Before discussing the numerical results, we begin with the proof of Eq. (18). For the Hamiltonian in Eq. (2), given that the density matrix of the ground state has a tensor product structure, and using Eq. (15), the logarithmic negativity

$$\mathcal{E} \left(\bigotimes_{\gamma} \rho_{\gamma}^{T_B^f} \right) = \sum_{\gamma} \mathcal{E} \left(\rho_{\gamma}^{T_B^f} \right). \quad (19)$$

Hence, one can analyze each $\rho_{\gamma}^{T_B^f}$ individually. We prove that the partially transposed density matrix ρ_{γ} in the overlap matrix approach is related to its counterpart in Fock space through a unitary transformation.

Proof. We expand the partially transposed single-mode density matrix in the overlap matrix approach $\rho_{\gamma}^{T_B^f}$ into Fock

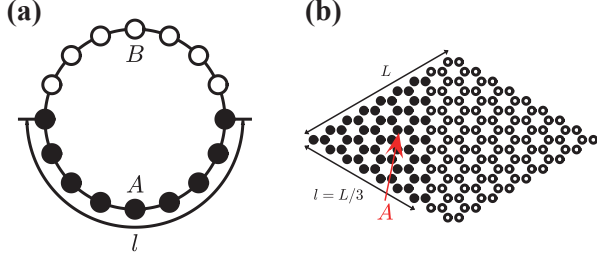


FIG. 1. Bipartite system for a chain and a honeycomb lattice. (a) A contiguous region A consisting of l sites is selected within a system of total size L . (b) For the honeycomb lattice, the system is partitioned such that one region forms a corner, with each edge consisting of $l = L/3$ unit cells. The entire system contains L unit cells along each lattice vector, allowing us to examine the scaling law in two dimensions.

space

$$\begin{aligned} \rho_{\gamma}^{T_B^f} &= \sum_{i \in A} \sum_{i' \in A} (UU)_{i\gamma} (\mathcal{U}^\dagger \mathcal{U}^\dagger)_{\gamma i'} c_i^\dagger |0\rangle \langle 0| c_{i'} \\ &+ \sum_{i \in B} \sum_{i' \in B} (UU)_{i\gamma} (\mathcal{U}^\dagger \mathcal{U}^\dagger)_{\gamma i'} c_i^\dagger |0\rangle \langle 0| c_{i'} \\ &- i \sum_{i \in A} \sum_{i' \in B} (\mathcal{U}^\dagger \mathcal{U}^\dagger)_{\gamma i} (\mathcal{U}^\dagger \mathcal{U}^\dagger)_{\gamma i'} |0\rangle \langle 0| c_{i'} c_i \\ &- i \sum_{i \in A} \sum_{i' \in B} (UU)_{i\gamma} (UU)_{i'\gamma} c_i^\dagger c_{i'}^\dagger |0\rangle \langle 0|. \end{aligned} \quad (20)$$

Comparing this with the density matrix partially transposed in Fock space, denoted as $\tilde{\rho}_{\gamma}^{T_B^f}$

$$\begin{aligned} \tilde{\rho}_{\gamma}^{T_B^f} &= \sum_{i \in A} \sum_{i' \in A} (UU)_{i\gamma} (\mathcal{U}^\dagger \mathcal{U}^\dagger)_{\gamma i'} c_i^\dagger |0\rangle \langle 0| c_{i'} \\ &+ \sum_{i \in B} \sum_{i' \in B} (UU)_{i\gamma} (\mathcal{U}^\dagger \mathcal{U}^\dagger)_{\gamma i'} c_i^\dagger |0\rangle \langle 0| c_{i'} \\ &- i \sum_{i \in A} \sum_{i' \in B} (UU)_{\gamma i'} (\mathcal{U}^\dagger \mathcal{U}^\dagger)_{\gamma i} |0\rangle \langle 0| c_{i'} c_i \\ &- i \sum_{i \in A} \sum_{i' \in B} (UU)_{i\gamma} (\mathcal{U}^\dagger \mathcal{U}^\dagger)_{i'\gamma} c_i^\dagger c_{i'}^\dagger |0\rangle \langle 0|, \end{aligned} \quad (21)$$

evidently, transforming $\tilde{\rho}_{\gamma}^{T_B^f}$ into $\rho_{\gamma}^{T_B^f}$ can be achieved through the unitary transformation $c_i \rightarrow e^{-2i \arg(\phi_{\gamma i})} c_i$, provided that $i \in B$ where $\phi_{\gamma i} = (UU)_{\gamma i}$.

Using Eq. (14), the identity $\mathcal{E} \left(\rho_{\gamma}^{T_B^f} \right) = \mathcal{E} \left(\tilde{\rho}_{\gamma}^{T_B^f} \right)$ holds, allowing us to compute bipartite negativity in free-fermion systems via the overlap matrix approach. In Appendix C, we verify the eigenvalues of Eq. (17) through exact diagonalization and obtain consistent results, indicating that a similarity transformation maps $\rho_{\gamma}^{T_B^f}$ to $\tilde{\rho}_{\gamma}^{T_B^f}$. This confirms that the overlap matrix can be effectively used to analyze the negative spectrum[50, 51]. Intriguingly, we find that the eigenvalues of $\rho_{\gamma}^{T_B^f}$ are either purely imaginary or real.

B. Two numerical examples

In the following, we consider two free fermion systems. The Hamiltonian we discuss here is

$$H = -\mu \sum_i c_i^\dagger c_i - t \sum_{\langle i, j \rangle} \left(c_i^\dagger c_j + \text{H.c.} \right), \quad (22)$$

where $\mu > 0$ is the chemical potential, and $\langle i, j \rangle$ denotes the nearest neighbor hopping, with $t > 0$ the hopping amplitude.

a. One-dimensional infinite chain. Consider an infinite lattice system ($L \rightarrow \infty$) with periodic boundary conditions (PBC), i.e. $c_{N+1} = c_1$. In a bipartite setup, as shown in Fig. 1(a), the overlap matrix takes the form of a Toeplitz matrix.

$$[M_A]_{\alpha, \beta} = L^{-1} \sum_{\nu=0}^{l-1} e^{i \frac{2\pi}{L} \nu (\beta - \alpha)}. \quad (23)$$

To obtain analytical results on entanglement, the formula in Eq. (18) should be generalized to a continuous form[46].

If we define the relation of the eigenvalues P_γ and its contribution to logarithmic negativity as $f(P_\gamma)$, i.e. $f(P_\gamma) = \ln \left(1 + 2\sqrt{P_\gamma(1-P_\gamma)} \right)$, then the logarithmic negativity formula becomes

$$\begin{aligned} \mathcal{E} &= \sum_{\gamma=1}^M f(P_\gamma) \\ &= \oint \frac{d\lambda}{2\pi i} \sum_{\gamma=1}^M \frac{f(\lambda)}{\lambda - P_\gamma} \\ &= \oint \frac{d\lambda}{2\pi i} f(\lambda) \frac{d \ln D_A(\lambda)}{d\lambda}, \end{aligned} \quad (24)$$

where the integral contour is shown in Fig. S2, and $D_A(\lambda) = \det \left(\tilde{M}_A - \lambda \mathbf{1} - M_A \right)$ represents the characteristic polynomial of the overlap matrix, which is also a Toeplitz matrix. The Fisher-Hartwig conjecture[6, 52–56] facilitates the evaluation of the determinant of the Toeplitz matrix \tilde{M}_A revealing that entanglement follows a volume law in a one-dimensional infinite chain (see Appendix B for a detailed derivation)

$$\begin{aligned} \mathcal{E} &\approx \frac{1}{\pi^2} \int_0^1 dx \frac{f(x)}{x(1-x)} \left[\ln L + \ln \left(2 \left| \sin \frac{1}{2} k_F \right| \right) \right] \\ &= \frac{1}{2} \left[\ln L + \ln \left(2 \left| \sin \frac{1}{2} k_F \right| \right) \right], \end{aligned} \quad (25)$$

where $k_F = \frac{l}{L} \cdot 2\pi$. When $l \ll L$, the logarithmic negativity follows $\mathcal{E} \sim \frac{1}{2} \ln l + C$, where C is a constant, consistent with Ref. [36, 37] for central charge $c = 1$. This is also supported by the numerical results in Fig. 2(a). For higher-dimensional systems, such as a hypercube lattice $[0, L_1] \times [0, L_2] \times \dots \times [0, L_d]$, the Widom conjecture[57] predicts that the entanglement scales as $\sim L^{d-1} \log L$ when region A is chosen as $[0, z_1 L] \times [0, z_2 L] \times \dots \times [0, z_d L]$ with $z_i < 1$ for $i = 1, \dots, d$. This result also aligns with previous studies[54, 58, 59].

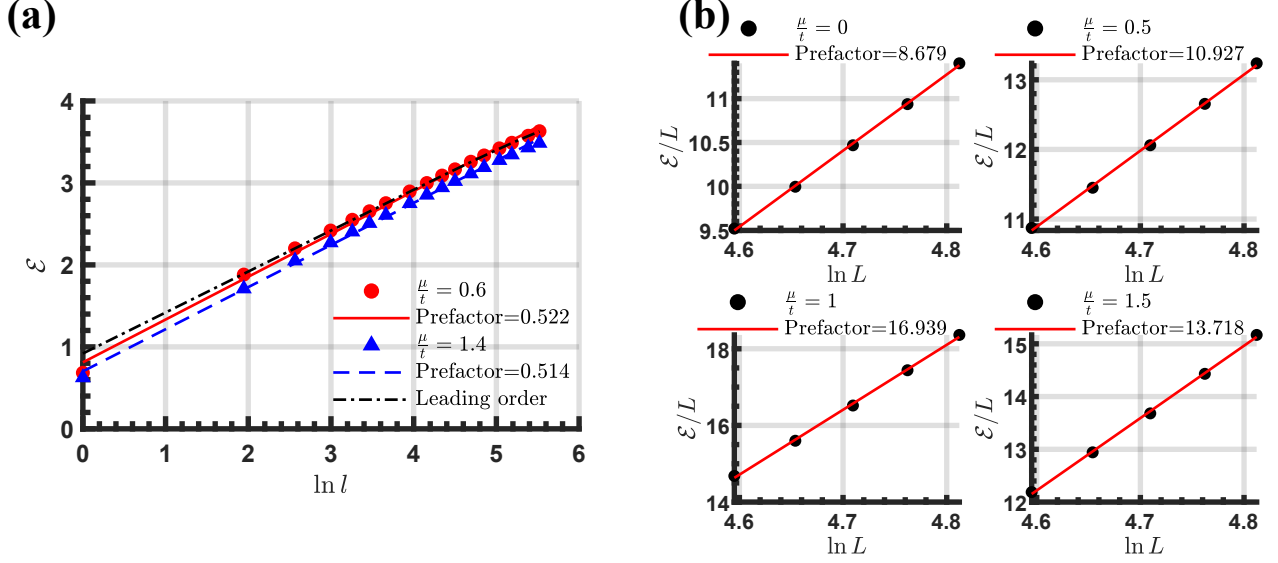


FIG. 2. Logarithmic negativity \mathcal{E} in different lattice systems. (a) \mathcal{E} as a function of $\ln l$ in a one-dimensional infinite chain for a bipartite system. The total chain length is set to 1000 sites. Two parameter choices are compared with the analytical formula (black line), both confirming the linear relationship between \mathcal{E} and the logarithm of the subsystem size. (b) \mathcal{E}/L versus $\ln L$ in a honeycomb lattice. The results indicate that logarithmic negativity follows the two-dimensional scaling law $\mathcal{E} \sim L \ln L$. The slope varies for different μ/t , reflecting changes in the Fermi surface.

b. Honeycomb lattice. From Fig. 2(b), the logarithmic negativity of the honeycomb lattice follows the scaling law $\sim L \log L$, suggesting that the Widom conjecture remains valid. The scaling factor varies depending on the shape and structure of the Fermi surface. This demonstrates that both examples are consistent with the Goev-Klich-Widom scaling law [57, 58, 60].

IV. LOGARITHMIC NEGATIVITY OF FREE FERMIONS SYSTEM IN TRIPARTITE CASE

Similar to Ref. [47], when the three overlap matrices M_{A_1} , M_{A_2} and M_B are simultaneously diagonalizable, the logarithmic negativity

$$\begin{aligned} \mathcal{E} = & \sum_{\gamma} \ln [P_{1\gamma} + P_{2\gamma} \\ & + \sqrt{\frac{1}{2} (P_{B\gamma}^2 + 2P_{1\gamma}P_{2\gamma} + P_{B\gamma}\sqrt{P_{B\gamma}^2 + 4P_{1\gamma}P_{2\gamma}})} \\ & + \sqrt{\frac{1}{2} (P_{B\gamma}^2 + 2P_{1\gamma}P_{2\gamma} - P_{B\gamma}\sqrt{P_{B\gamma}^2 + 4P_{1\gamma}P_{2\gamma}})}], \end{aligned} \quad (26)$$

where $P_{B\gamma}$ represents the probability of the γ -th particle in region B . It is worth noting that the complexity of this formula arises from the non-Hermitian nature of $\rho_{A_1}^f$ and simplifies to Eq. (18) when region B contains no lattice sites, leading to $P_{B\gamma} = 0$ for all γ .

When three overlap matrices cannot be simultaneously diagonalized, rather than dealing with the complexity of deriving ρ_A , it is more convenient to begin the tripartite entanglement negativity calculation from Eq. (10). However, this

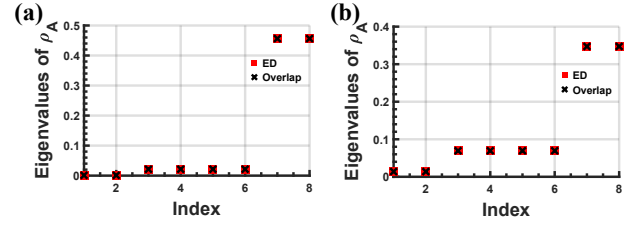


FIG. 3. Comparison of the eigenvalues of ρ_A , after reordering and removing the zero components, between the partial trace in overlap matrix approach and in Fock space. We consider an $N = 12$ and $\mu/t = 1$ homogeneous one-dimensional chain in two bipartite geometries: (a) an adjacent interval case where the system is evenly divided into regions A and B ; (b) a disjoint interval case where the system is evenly partitioned into A_1, B_1, A_2 and B_2 sequentially.

equation should be considered rigorously, as the eigenvalues of ρ_A have not yet been verified.

A. Overlap matrix approach preserves the eigenvalues of ρ_A

In this subsection, we compare the eigenvalues of Eq. (10) with exact diagonalization results. We consider two types of tripartite geometries: adjacent intervals and disjoint intervals. As shown in Fig. 3, both geometries yield identical eigenvalues for the partial trace in different representations. Additionally, the reduced density matrix has no more than 2^M nonzero eigenvalues contributing to the entanglement. This result further demonstrates that reduced density matrices in the overlap matrix approach and Fock space are related by a

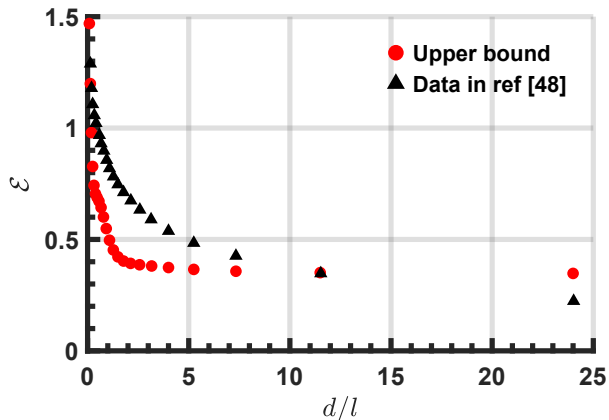


FIG. 4. Comparison of the logarithmic negativity in Ref. [47] with its upper bound in the $M = 5$ case, highlighting the necessity of a careful approach in the partial transposition procedure.

unitary transformation, a property that does not always hold in the Jordan-Wigner transformation [61–63].

The key reason behind the validity of the partial trace in the overlap matrix approach lies in its “semi-local” nature, meaning that it remains associated with either region A or B . Consequently, tracing out region A or B does not lead to the loss of information about the remaining region. A general proof in Appendix D and the numerical benchmark confirm that the entanglement spectrum [64–67] can be reliably obtained using the overlap matrix approach.

B. Logarithmic negativity for tripartite system

Previous studies [47] faced an exponential complexity issue in calculating logarithmic negativity when three overlap matrices could not be simultaneously diagonalized. The Green’s function approach provides an upper bound for the logarithmic negativity of free fermion systems in the bPT framework. Using this method, we find that although the numerical results in Ref. [47] capture the entanglement scaling law, they violate this upper bound. The upper bound of the mixed-state logarithmic negativity [1, 37–39]

$$\mathcal{E}\left(\rho_A^{T_{A_1}^b}\right) \leq \mathcal{E}\left(\rho_A^{T_{A_1}^f}\right) + \ln \sqrt{2}, \quad (27)$$

where $\rho_A^{T_{A_1}^b}$ represents the reduced density matrix after bPT. In Fig. 4, we demonstrate that the logarithmic negativity reported in Ref. [47] exceeds the upper bound in the $M = 5$ case.

Our clarification is as follows: while $\tilde{\rho}_B^{T_B^f}$ in overlap matrix approach connects to $\rho_B^{T_B^f}$ in Fock space via a similarity transformation for pure states, this does not hold for mixed states, which are classical mixtures of pure states. The transformations of different pure states vary, meaning that their classical mixtures disrupts the similarity transformation between $\tilde{\rho}_B^{T_B^f}$

and $\rho_B^{T_B^f}$. As a result, the findings in Ref. [47] are not totally exact.

V. CONCLUSIONS

In this study, we have presented a detailed analysis of the overlap matrix approach for computing entanglement in free-fermion systems, with a particular emphasis on the partial trace and fermionic partial transpose operations within the overlap matrix framework. In the bipartite case, we demonstrated that for pure states, the eigenvalues of ρ_A remain invariant under the overlap matrix approach. This property establishes the overlap matrix approach as the first known “semi-global” mapping capable of preserving the eigenvalues of ρ_A , providing a significant advantage in entanglement computations. Moreover, we derived an analytical formula for the bipartite logarithmic negativity, offering a concise and computationally efficient method for quantifying entanglement in such systems.

For mixed states, however, the situation is more complex. Using tripartite geometries as a representative example, we identified a critical limitation in the overlap matrix mapping: the logarithmic negativity reported in Ref. [47] exceeds the theoretical upper bound. This discrepancy arises because the partial transpose operation in the overlap matrix mapping preserves eigenvalues only for pure states. For mixed states, which are classical mixtures of pure states, this equivalence breaks down due to the inconsistent transformations of individual pure states under the overlap matrix approach. This finding underscores the need for careful consideration when applying overlap matrix approach in the context of mixed states.

In summary, our work highlights both the strengths and limitations of the overlap matrix approach. For bipartite entanglement, this method proves to be a more effective and reliable strategy compared to the Green’s function approach, particularly due to its ability to preserve eigenvalues under “semi-local” mappings. However, the framework for tripartite entanglement remains incomplete, as the overlap matrix approach encounters challenges when applied to mixed states. In this context, the Green’s function approach remains the preferred choice for numerical studies due to its broader applicability.

Beyond these specific findings, our study introduces a novel perspective on entanglement research. We have demonstrated that the partial trace operation in overlap matrix approach preserves the eigenvalues of the reduced density matrix, a property that has important implications for future research. This insight provides a foundation for further refinement and application of the overlap matrix approach, potentially advancing the field of entanglement computation in free-fermion systems.

Acknowledgments— We thank Fo-Hong Wang for helpful discussion. This work was supported by the National Natural Science Foundation of China (Grants No. 12447103, No. 12274289), the National Key R&D Program of China (Grant No. 2022YFA1402702, No. 2021YFA1401400), the Innovation Program for Quantum Science and Technology (under

Grant No. 2021ZD0301902), Yangyang Development Fund, and startup funds from SJTU. The computations in this pa-

per were run on the Siyuan-1 and π 2.0 clusters supported by the Center for High Performance Computing at Shanghai Jiao Tong University.

-
- [1] H. Shapourian, K. Shiozaki, and S. Ryu, Partial time-reversal transformation and entanglement negativity in fermionic systems, *Phys. Rev. B* **95**, 165101 (2017).
- [2] G. Vidal, J. I. Latorre, E. Rico, and A. Kitaev, Entanglement in quantum critical phenomena, *Phys. Rev. Lett.* **90**, 227902 (2003).
- [3] L. Amico, R. Fazio, A. Osterloh, and V. Vedral, Entanglement in many-body systems, *Rev. Mod. Phys.* **80**, 517 (2008).
- [4] N. Laflorencie, Quantum entanglement in condensed matter systems, *Physics Reports* **646**, 1 (2016), quantum entanglement in condensed matter systems.
- [5] P. Calabrese and J. Cardy, Entanglement entropy and conformal field theory, *Journal of Physics A: Mathematical and Theoretical* **42**, 504005 (2009).
- [6] J. Eisert, M. Cramer, and M. B. Plenio, Colloquium: Area laws for the entanglement entropy, *Rev. Mod. Phys.* **82**, 277 (2010).
- [7] A. Osterloh, L. Amico, G. Falci, and R. Fazio, Scaling of entanglement close to a quantum phase transition, *Nature* **416**, 608 (2002).
- [8] A. Kitaev and J. Preskill, Topological entanglement entropy, *Phys. Rev. Lett.* **96**, 110404 (2006).
- [9] M. Levin and X.-G. Wen, Detecting topological order in a ground state wave function, *Phys. Rev. Lett.* **96**, 110405 (2006).
- [10] T.-C. Lu and T. Grover, Singularity in entanglement negativity across finite-temperature phase transitions, *Phys. Rev. B* **99**, 075157 (2019).
- [11] P. Calabrese, J. Cardy, and B. Doyon, Entanglement entropy in extended quantum systems, *Journal of Physics A: Mathematical and Theoretical* **42**, 500301 (2009).
- [12] H.-C. Jiang, Z. Wang, and L. Balents, Identifying topological order by entanglement entropy, *Nature Physics* **8**, 902 (2012).
- [13] R. Horodecki, P. Horodecki, M. Horodecki, and K. Horodecki, Quantum entanglement, *Rev. Mod. Phys.* **81**, 865 (2009).
- [14] G. Vidal and R. F. Werner, Computable measure of entanglement, *Phys. Rev. A* **65**, 032314 (2002).
- [15] M. B. Plenio, Logarithmic negativity: A full entanglement monotone that is not convex, *Phys. Rev. Lett.* **95**, 090503 (2005).
- [16] S. Parker and M. B. Plenio, Entanglement simulations of shor's algorithm, *Journal of Modern Optics* **49**, 1325 (2002), <https://doi.org/10.1080/09500340110107207>.
- [17] A. Peres, Separability criterion for density matrices, *Phys. Rev. Lett.* **77**, 1413 (1996).
- [18] M. Horodecki, P. Horodecki, and R. Horodecki, Separability of mixed states: necessary and sufficient conditions, *Physics Letters A* **223**, 1 (1996).
- [19] K. Audenaert, J. Eisert, M. B. Plenio, and R. F. Werner, Entanglement properties of the harmonic chain, *Phys. Rev. A* **66**, 042327 (2002).
- [20] V. Eisler and Z. Zimborás, Entanglement negativity in the harmonic chain out of equilibrium, *New Journal of Physics* **16**, 123020 (2014).
- [21] A. Ferraro, D. Cavalcanti, A. García-Saez, and A. Acín, Thermal bound entanglement in macroscopic systems and area law, *Phys. Rev. Lett.* **100**, 080502 (2008).
- [22] C. D. Nobili, A. Coser, and E. Tonni, Entanglement negativity in a two dimensional harmonic lattice: area law and corner contributions, *Journal of Statistical Mechanics: Theory and Experiment* **2016**, 083102 (2016).
- [23] A. Bayat, S. Bose, and P. Sodano, Entanglement routers using macroscopic singlets, *Phys. Rev. Lett.* **105**, 187204 (2010).
- [24] A. Bayat, P. Sodano, and S. Bose, Negativity as the entanglement measure to probe the kondo regime in the spin-chain kondo model, *Phys. Rev. B* **81**, 064429 (2010).
- [25] A. Bayat, S. Bose, P. Sodano, and H. Johannesson, Entanglement probe of two-impurity kondo physics in a spin chain, *Phys. Rev. Lett.* **109**, 066403 (2012).
- [26] H. Wichterich, J. Vidal, and S. Bose, Universality of the negativity in the lipkin-meshkov-glick model, *Phys. Rev. A* **81**, 032311 (2010).
- [27] H. Wichterich, J. Molina-Vilaplana, and S. Bose, Scaling of entanglement between separated blocks in spin chains at criticality, *Phys. Rev. A* **80**, 010304 (2009).
- [28] M. B. Hastings, I. González, A. B. Kallin, and R. G. Melko, Measuring renyi entanglement entropy in quantum monte carlo simulations, *Phys. Rev. Lett.* **104**, 157201 (2010).
- [29] R. A. Santos, V. Korepin, and S. Bose, Negativity for two blocks in the one-dimensional spin-1 affleck-kennedy-lieb-tasaki model, *Phys. Rev. A* **84**, 062307 (2011).
- [30] K.-H. Wu, T.-C. Lu, C.-M. Chung, Y.-J. Kao, and T. Grover, Entanglement renyi negativity across a finite temperature transition: A monte carlo study, *Phys. Rev. Lett.* **125**, 140603 (2020).
- [31] C. Castelnovo, Negativity and topological order in the toric code, *Phys. Rev. A* **88**, 042319 (2013).
- [32] Y. A. Lee and G. Vidal, Entanglement negativity and topological order, *Phys. Rev. A* **88**, 042318 (2013).
- [33] T.-C. Lu, T. H. Hsieh, and T. Grover, Detecting topological order at finite temperature using entanglement negativity, *Phys. Rev. Lett.* **125**, 116801 (2020).
- [34] P. Calabrese, J. Cardy, and E. Tonni, Entanglement negativity in extended systems: a field theoretical approach, *Journal of Statistical Mechanics: Theory and Experiment* **2013**, P02008 (2013).
- [35] P. Calabrese, J. Cardy, and E. Tonni, Entanglement negativity in quantum field theory, *Phys. Rev. Lett.* **109**, 130502 (2012).
- [36] P. Calabrese, J. Cardy, and E. Tonni, Finite temperature entanglement negativity in conformal field theory, *Journal of Physics A: Mathematical and Theoretical* **48**, 015006 (2014).
- [37] H. Shapourian and S. Ryu, Finite-temperature entanglement negativity of free fermions, *Journal of Statistical Mechanics: Theory and Experiment* **2019**, 043106 (2019).
- [38] V. Eisler and Z. Zimborás, On the partial transpose of fermionic gaussian states, *New Journal of Physics* **17**, 053048 (2015).
- [39] J. Eisert, V. Eisler, and Z. Zimborás, Entanglement negativity bounds for fermionic gaussian states, *Phys. Rev. B* **97**, 165123 (2018).
- [40] K. Shiozaki, H. Shapourian, K. Gomi, and S. Ryu, Many-body topological invariants for fermionic short-range entangled topological phases protected by antiunitary symmetries, *Phys. Rev. B* **98**, 035151 (2018).
- [41] H. Shapourian and S. Ryu, Entanglement negativity of fermions: Monotonicity, separability criterion, and classifica-

- tion of few-mode states, *Phys. Rev. A* **99**, 022310 (2019).
- [42] F.-H. Wang and X. Y. Xu, Entanglement rényi negativity of interacting fermions from quantum monte carlo simulations (2024), [arXiv:2312.14155](https://arxiv.org/abs/2312.14155) [cond-mat.str-el].
- [43] H. Shapourian, P. Ruggiero, S. Ryu, and P. Calabrese, Twisted and untwisted negativity spectrum of free fermions, *SciPost Phys.* **7**, 037 (2019).
- [44] F.-H. Wang and X. Y. Xu, Untwisted and twisted rényi negativities: Toward a rényi proxy for logarithmic negativity in fermionic systems (2025), [arXiv:2503.07731](https://arxiv.org/abs/2503.07731) [cond-mat.str-el].
- [45] I. Klich, Lower entropy bounds and particle number fluctuations in a fermi sea, *Journal of Physics A: Mathematical and General* **39**, L85 (2006).
- [46] P. Calabrese, M. Mintchev, and E. Vicari, Entanglement entropy of one-dimensional gases, *Phys. Rev. Lett.* **107**, 020601 (2011).
- [47] P.-Y. Chang and X. Wen, Entanglement negativity in free-fermion systems: An overlap matrix approach, *Phys. Rev. B* **93**, 195140 (2016).
- [48] P.-Y. Chang, J.-S. You, X. Wen, and S. Ryu, Entanglement spectrum and entropy in topological non-hermitian systems and nonunitary conformal field theory, *Phys. Rev. Res.* **2**, 033069 (2020).
- [49] A. Ossipov, Entanglement entropy in fermi gases and anderson's orthogonality catastrophe, *Phys. Rev. Lett.* **113**, 130402 (2014).
- [50] P. Ruggiero, V. Alba, and P. Calabrese, Negativity spectrum of one-dimensional conformal field theories, *Phys. Rev. B* **94**, 195121 (2016).
- [51] S. Murciano, V. Vitale, M. Dalmonte, and P. Calabrese, Negativity hamiltonian: An operator characterization of mixed-state entanglement, *Phys. Rev. Lett.* **128**, 140502 (2022).
- [52] M. E. Fisher and R. E. Hartwig, Toeplitz determinants: Some applications, theorems, and conjectures, in *Advances in Chemical Physics* (John Wiley & Sons, Ltd, 1969) pp. 333–353, <https://onlinelibrary.wiley.com/doi/pdf/10.1002/9780470143605.ch18>.
- [53] Jin, B.-Q., Korepin, and E. V., Quantum spin chain, toeplitz determinants and the fisher–hartwig conjecture., *Journal of Statistical Physics* (2004).
- [54] S. Fraenkel and M. Goldstein, Symmetry resolved entanglement: exact results in 1d and beyond, *Journal of Statistical Mechanics: Theory and Experiment* **2020**, 033106 (2020).
- [55] E. L. Basor and K. E. Morrison, The fisher-hartwig conjecture and toeplitz eigenvalues, *Linear Algebra and its Applications* **202**, 129 (1994).
- [56] F. Franchini and A. G. Abanov, Asymptotics of toeplitz determinants and the emptiness formation probability for the xy spin chain, *Journal of Physics A: Mathematical and General* **38**, 5069 (2005).
- [57] H. Widom, On a class of integral operators with discontinuous symbol, in *Toeplitz Centennial: Toeplitz Memorial Conference in Operator Theory, Dedicated to the 100th Anniversary of the Birth of Otto Toeplitz, Tel Aviv, May 11–15, 1981*, edited by I. Gohberg (Birkhäuser Basel, Basel, 1982) pp. 477–500.
- [58] D. Gioev and I. Klich, Entanglement entropy of fermions in any dimension and the widom conjecture, *Phys. Rev. Lett.* **96**, 100503 (2006).
- [59] Calabrese, P., Mintchev, M., and Vicari, E., Entanglement entropies in free-fermion gases for arbitrary dimension, *EPL* **97**, 20009 (2012).
- [60] Z.-K. Lin, Y. Zhou, B. Jiang, B.-Q. Wu, L.-M. Chen, X.-Y. Liu, L.-W. Wang, P. Ye, and J.-H. Jiang, Measuring entanglement entropy and its topological signature for phononic systems, *Nature Communications* **15**, 1601 (2024).
- [61] F. Iglói and I. Peschel, On reduced density matrices for disjoint subsystems, *Europhysics Letters* **89**, 40001 (2010).
- [62] N. Friis, Reasonable fermionic quantum information theories require relativity, *New Journal of Physics* **18**, 033014 (2016).
- [63] J. Surace and L. Tagliacozzo, Fermionic Gaussian states: an introduction to numerical approaches, *SciPost Phys. Lect. Notes* , 54 (2022).
- [64] P. Calabrese and A. Lefevre, Entanglement spectrum in one-dimensional systems, *Phys. Rev. A* **78**, 032329 (2008).
- [65] F. F. Assaad, T. C. Lang, and F. Parisen Toldin, Entanglement spectra of interacting fermions in quantum monte carlo simulations, *Phys. Rev. B* **89**, 125121 (2014).
- [66] C. H. Lee and P. Ye, Free-fermion entanglement spectrum through wannier interpolation, *Phys. Rev. B* **91**, 085119 (2015).
- [67] M. Hermanns, Y. Salimi, M. Haque, and L. Fritz, Entanglement spectrum and entanglement hamiltonian of a chern insulator with open boundaries, *Journal of Statistical Mechanics: Theory and Experiment* **2014**, P10030 (2014).

Appendix A: Supplementary material on the bipartite overlap matrix approach

a. The range of eigenvalues of overlap matrix. Here, we will prove that the eigenvalues of the overlap matrix lie within the range $[0, 1]$. To demonstrate this, it is convenient to adopt the wave function representation. After a unitary diagonalization, the overlap matrix takes the form

$$\begin{aligned} [\mathcal{U}M_A\mathcal{U}^\dagger]_{\alpha\beta} &= \sum_{k,k'} \mathcal{U}_{\alpha k} [M_A]_{kk'} [\mathcal{U}^\dagger]_{k'\beta} \\ &= \sum_{kk'} \int_{\mathbf{r} \in A} \mathcal{U}_{\alpha k} \phi_k^*(\mathbf{r}) \phi_{k'}(\mathbf{r}) [\mathcal{U}^\dagger]_{k'\beta} d\mathbf{r}. \end{aligned} \quad (\text{A1})$$

A new set of eigenstates $\psi_\alpha = \sum_k [\mathcal{U}^\dagger]_{k\alpha} \phi_k(\mathbf{r})$ is constructed, preserving both orthogonality and normalization. Consequently, the integral of the squared modulus ψ_α over region A cannot exceed 1.

b. The eigenvalues of $\tilde{\rho}_i^{T_B^f}$. Here we will prove that the eigenvalues of $\tilde{\rho}_i^{T_B^f}$ in Eq. (20) are identical to those of $\rho_i^{T_B^f}$ in Eq. (21). By rearranging the basis order, both matrices can be block diagonalized into the form shown in Fig. S1. The first two blocks, which contain nonzero elements (i.e. the red and orange blocks), are completely identical in both density matrices. Therefore, we only need to analyze the characteristic polynomial of the yellow block.

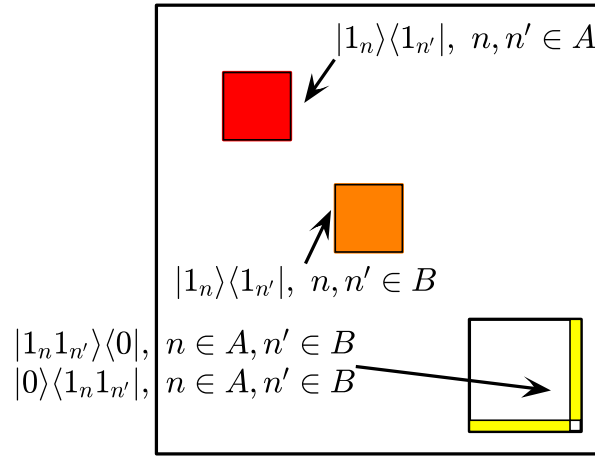


FIG. S1. The block diagonal structure of $\tilde{\rho}_i^{T_B^f}$ and $\rho_i^{T_B^f}$.

The characteristic polynomial has a general form

$$\begin{aligned} \det \begin{pmatrix} -\lambda & & & b_1 \\ & -\lambda & & b_2 \\ & & \ddots & \vdots \\ a_1 & a_2 & \cdots & a_{N-1} & -\lambda \end{pmatrix} &= -\lambda \det \begin{pmatrix} -\lambda & & & b_2 \\ & \ddots & & \vdots \\ & & \ddots & b_{N-1} \\ a_2 & \cdots & a_{N-1} & -\lambda \end{pmatrix} + (-1)^N a_1 \det \begin{pmatrix} -\lambda & & & b_1 \\ & \ddots & & \vdots \\ & & \ddots & -\lambda & b_{N-1} \end{pmatrix} \\ &= -\lambda \det \begin{pmatrix} -\lambda & & & b_2 \\ & \ddots & & \vdots \\ & & \ddots & b_{N-1} \\ a_2 & \cdots & a_{N-1} & -\lambda \end{pmatrix} + (-1)^{2N-1} a_1 b_1 \det \begin{pmatrix} -\lambda & & & \\ & \ddots & & \\ & & \ddots & -\lambda \end{pmatrix} \\ &= \cdots \\ &= (-1)^{2N-1} (-\lambda)^{N-2} a_1 b_1 + (-1)^{2N-3} (-\lambda)^{N-2} a_2 b_2 + \cdots + (-1)^{2-2-1} (-\lambda)^{N-2} a_{N-1} b_{N-1} \\ &\equiv f(a_1 b_1; a_2 b_2, \cdots, a_{N-1} b_{N-1}). \end{aligned} \quad (\text{A2})$$

This demonstrates that the characteristic polynomial depends on the sequence $\{a_1b_1, a_2b_2, \dots, a_{N-1}b_{N-1}\}$. Evidently, the values of a_ib_i in $\rho_i^{T_B^f}$ are identical to those in $\tilde{\rho}_i^{T_B^f}$. Consequently, the characteristic polynomial and the eigenvalues remain unchanged.

Appendix B: The Fisher-Hartwig conjecture

Following Ref. [53], we now proceed with the proof of Eq. (25).

In Eq. (23) the overlap matrix is a Toeplitz matrix which indicates that the matrix elements $[M_A]_{i,j}$ depend only on the value of $i - j$, i.e. $[M_A]_{i,j} = f(i - j)$ where the function f depends on the specific context. The Toeplitz matrix, denoted as $T_L[\phi]$ in general, is generated by a function $\phi(\theta)$ if its entries are given by the Fourier coefficients of $\phi(\theta)$

$$T_L[\phi] = \frac{1}{2\pi} \int_0^{2\pi} \phi(\theta) e^{-i(i-j)\theta} d\theta, \quad i, j = 1, \dots, L - 1 \quad (\text{B1})$$

In our case the overlap matrix

$$\begin{aligned} \phi_l &\approx \int_{-\frac{1}{2} + \frac{l}{L}}^{\frac{1}{2}} e^{-i2\pi l\nu} d\nu \\ &= \frac{1}{2\pi} \int_{-\pi + \frac{l}{L} \cdot 2\pi}^{\pi} e^{-il\nu} d\nu \\ &= \frac{1}{2\pi} e^{il\pi} \int_0^{2\pi} \phi(\theta) e^{-il\theta} d\theta, \end{aligned} \quad (\text{B2})$$

where

$$\phi(\theta) = \begin{cases} 0 & \text{if } \theta \in [0, k_F] \\ 1 & \text{if } \theta \in [k_F, 2\pi] \end{cases}, \quad k_F = \frac{l}{L} \cdot 2\pi \quad (\text{B3})$$

For the Toeplitz matrix $\tilde{M}_A = \lambda \mathbf{1} - M_A$, the generating function is obtained by replacing 0 with λ and 1 with $\lambda - 1$ respectively. Regarding the singularities of the generating function, it can be decomposed into a product of functions with known asymptotic behavior, which facilitates the application of the Fisher-Hartwig conjecture

$$\phi(\theta) = \psi(\theta) \prod_{r=1}^R t_{\beta_r, \theta_r}(\theta) u_{\alpha_r, \theta_r}(\theta), \quad (\text{B4})$$

where

$$\begin{aligned} t_{\beta_r, \theta_r}(\theta) &= \exp[-i\beta_r(\pi - \theta + \theta_r)], \quad \theta_r < \theta < 2\pi + \theta_r \\ u_{\alpha_r, \theta_r}(\theta) &= (2 - 2\cos(\theta - \theta_r))^{\alpha_r}. \quad \text{Re } \alpha_r > -\frac{1}{2} \end{aligned} \quad (\text{B5})$$

In our case, the jump discontinuity of the generating function is characterized by $R = 2$, with parameters $\beta = -\beta_1 = \beta_2 = \frac{1}{2\pi i} \ln \frac{\lambda-1}{\lambda}$, and the singular points located at $\theta_1 = k_F$ and $\theta_2 = 0$. The smooth part of the generating function is given by

$$\psi(\theta) = (\lambda - 1) \left(\frac{\lambda-1}{\lambda} \right)^{-\frac{k_F}{2\pi}}.$$

Then the Fisher-Hartwig conjecture illustrates that the determinant of a Toeplitz matrix

$$D_L = (\mathcal{F}[\psi])^L \left(\prod_{i=1}^R L^{\alpha_i^2 - \beta_i^2} \right) \mathcal{E}[\psi, \{\alpha_i\}, \{\beta_i\}, \{\theta_i\}] \quad \text{when } L \rightarrow \infty \quad (\text{B6})$$

$$\mathcal{F}[\psi] = \exp \left[\frac{1}{2\pi} \int_0^{2\pi} \ln \psi(\theta) d\theta \right] \quad (\text{B7})$$

$$\begin{aligned}
\mathcal{E}[\psi, \{\alpha_i\}, \{\beta_i\}, \{\theta_i\}] &= \mathcal{E}[\psi] \\
&\times \prod_{i=1}^R G(1 + \alpha_i + \beta_i) G(1 + \alpha_i - \beta_i) / G(1 + 2\alpha_i) \\
&\times \prod_{i=1}^R (\psi_-(\exp(i\theta_i)))^{-\alpha_i - \beta_i} (\psi_+(\exp(-i\theta_i)))^{-\alpha_i + \beta_i} \\
&\times \prod_{1 \leq i \neq j \leq R} (1 - \exp(i(\theta_i - \theta_j)))^{-(\alpha_i + \beta_i)(\alpha_j - \beta_j)}
\end{aligned} \tag{B8}$$

$$\mathcal{E}[\psi] = \exp \left[\sum_{k=1}^{\infty} k s_k s_{-k} \right] \tag{B9}$$

$$G(1 + z) = (2\pi)^{z/2} e^{-(z+1)z/2 - \gamma_E z^2/2} \prod_{n=1}^{\infty} \{(1 + z/n)^n e^{-z + z^2/(2n)}\}, \tag{B10}$$

where s_k represents the k th Fourier coefficient of $\ln \psi(\theta)$. In our case since $\psi(\theta)$ is a constant independent of θ , we temporarily denote it as C , leading to $s_k = C\delta(k)$. Consequently, the summation simplifies as follows $\sum_{k=1}^{\infty} k s_k s_{-k} \rightarrow \int_0^{\infty} C^2 k \delta(k) \delta(-k) dk = 0$. By substituting Eq. (B7), Eq. (B8), Eq. (B9), and Eq. (B10) into Eq. (B6), we arrive at the desired result.

$$\begin{aligned}
D_L(\lambda) &= \left[(\lambda - 1) \left(\frac{\lambda - 1}{\lambda} \right)^{-\frac{k_F}{2\pi}} \right]^L L^{-2\beta^2(\lambda)} \\
&\quad e^{-(1+\gamma_E)\beta^2(\lambda)} \prod_{n=1}^{\infty} \left[\left(1 - \frac{\beta^2(\lambda)}{n^2} \right)^n e^{\frac{\beta^2(\lambda)}{n^2}} \right] \\
&\quad (2 - 2 \cos k_F)^{-\beta^2(\lambda)},
\end{aligned} \tag{B11}$$

and

$$\begin{aligned}
\frac{d \ln D_L(\lambda)}{d\lambda} &= L \left[\frac{1}{\lambda - 1} - \frac{k_F}{2\pi} \left(\frac{1}{\lambda - 1} - \frac{1}{\lambda} \right) \right] \\
&\quad - \left(2 \ln L + (1 + \gamma_E) + \sum_{n=1}^{\infty} \left[\frac{n}{n^2 - \beta^2(\lambda)} - \frac{1}{n} \right] + \ln(2 - 2 \cos k_F) \right) \frac{d\beta^2(\lambda)}{d\lambda} \\
&= L \left[\frac{1}{\lambda - 1} - \frac{k_F}{2\pi} \left(\frac{1}{\lambda - 1} - \frac{1}{\lambda} \right) \right] \\
&\quad - \frac{2\beta(\lambda)}{\pi i \lambda (\lambda - 1)} \left[\ln L + (1 + \gamma_E) + \ln(2 |\sin \frac{1}{2} k_F|) + \Upsilon(\lambda) \right],
\end{aligned} \tag{B12}$$

where $\Upsilon(\lambda) = \sum_{n=1}^{\infty} \frac{n}{n^2 - \beta^2(\lambda)} - \frac{1}{n}$. For the linear term in L , since all of them exist a first-order pole in λ , the integral over λ ultimately contributes zero to them based on the residue theorem. Therefore, the entanglement quantity is given by

$$\text{Entanglement quantity} = \frac{1}{\pi^2} \oint d\lambda f(\lambda) \frac{\beta(\lambda)}{\lambda(\lambda - 1)} \left[\ln L + (1 + \gamma_E) + \ln(2 |\sin \frac{1}{2} k_F|) + \Upsilon(\lambda) \right], \tag{B13}$$

where the integral contour is shown in Fig. S2. The residue theorem ensures that the contributions from the integration paths \overrightarrow{FED} and \overrightarrow{CAB} vanish. Consequently, the integral simplifies to

$$\begin{aligned}
\text{Entanglement quantity} &= \frac{1}{\pi^2} \left(\int_{1+i0^+}^{0+i0^+} + \int_{0+i0^-}^{1+i0^-} \right) d\lambda f(\lambda) \frac{\beta(\lambda)}{\lambda(\lambda - 1)} \\
&\quad \left[\ln L + (1 + \gamma_E) + \ln(2 |\sin \frac{1}{2} k_F|) + \Upsilon(\lambda) \right].
\end{aligned} \tag{B14}$$

In the complex number field the phase of $\beta(\lambda)$ must be taken into account to ensure a consistent and well-defined formulation

$$\begin{aligned}\beta(x(\in \mathbb{R}) + i0^\pm) &= \frac{1}{2\pi i} \left(\text{Ln} \frac{(x-1+i0^\pm)(x-i0^\pm)}{x^2} \right) \\ &= -iW(x) + \left(\frac{1}{2} - 0^\pm \right),\end{aligned}\tag{B15}$$

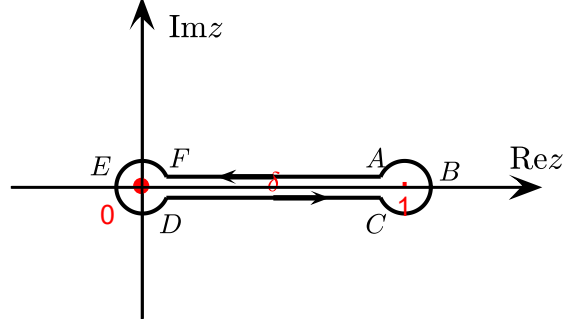


FIG. S2. The integral contour in Eq. (B13) consists of arcs \overrightarrow{FED} and \overrightarrow{CBA} with radii $\epsilon \rightarrow 0$. The midpoint of these arcs originate from the range of eigenvalues of the overlap matrix. The imaginary part of $\overrightarrow{AF}(\overrightarrow{DC})$ is given by $\delta = 0^+$ ($-\delta = 0^-$).

where $W(x) = \frac{1}{2\pi} \ln \frac{1-x}{x}$. Then the integral

$$\begin{aligned}\text{Entanglement quantity} &= \frac{-1}{\pi^2} \int_0^1 dx \frac{f(x)}{x(x-1)} \left[\ln L + (1 + \gamma_E) + \ln \left(2 \left| \sin \frac{1}{2} k_F \right| \right) \right] \\ &+ \frac{1}{\pi^2} \sum_{n=1}^{\infty} \int_0^1 dx \frac{f(x)}{x(x-1)} n \left[\frac{iW(x) - \frac{1}{2}}{n^2 - [-iW(x) + \frac{1}{2}]^2} \right. \\ &\quad \left. + \frac{-iW(x) - \frac{1}{2}}{n^2 - [-\frac{1}{2} - iW(x)]^2} + \frac{1}{n^2} \right] \\ &\equiv E_1 + E_2.\end{aligned}\tag{B16}$$

Introduce the ψ function

$$\psi(x) \equiv \frac{d}{dx} \ln \Gamma(x) = -\gamma_E + \sum_{n=0}^{\infty} \frac{1}{n+1} - \sum_{n=0}^{\infty} \frac{1}{n+x},\tag{B17}$$

with the property $\psi(x+1) = \psi(x) + \frac{1}{x}$, the infinite series is simplified as

$$\begin{aligned}E_2 &= \frac{1}{\pi^2} \int_0^1 dx \frac{f(x)}{x(x-1)} (-1) \left[-\gamma_E + \sum_{n=0}^{\infty} \frac{1}{n+1} - \sum_{n=1}^{\infty} \frac{1}{n} \right. \\ &\quad \left. - \frac{1}{2} \left(\psi\left(\frac{1}{2} - iW(x)\right) + \psi\left(\frac{1}{2} + iW(x)\right) \right) - 1 \right] \\ &= \frac{-1}{\pi^2} \int_0^1 dx \frac{f(x)}{x(x-1)} (-\gamma_E - 1) \\ &+ \frac{1}{2\pi^2} \int_0^1 dx \frac{f(x)}{x(x-1)} \left[\psi\left(\frac{1}{2} - iW(x)\right) + \psi\left(\frac{1}{2} + iW(x)\right) \right].\end{aligned}\tag{B18}$$

The first line of E_2 cancels out with E_1 , leaving the entanglement quantity as

$$\begin{aligned} \text{Entanglement quantity} &= \frac{-1}{\pi^2} \int_0^1 dx \frac{f(x)}{x(x-1)} \left[\ln L + \ln \left(2 \left| \sin \frac{1}{2} k_F \right| \right) \right] \\ &+ \frac{1}{2\pi^2} \int_0^1 dx \frac{f(x)}{x(x-1)} \left[\psi \left(\frac{1}{2} - iW(x) \right) + \psi \left(\frac{1}{2} + iW(x) \right) \right]. \end{aligned} \quad (\text{B19})$$

The first line precisely corresponds to Eq. (25), while the second line represents the next-to-leading order correction term.

Appendix C: The eigenvalues of the density matrix after partial transpose in the overlap matrix approach

In this appendix, we will generalize our result to a random hopping model, i.e.

$$H = \sum_{i,j} t_{ij} c_i^\dagger c_j = \mathbf{c}^\dagger \mathbf{t} \mathbf{c}, \quad (\text{C1})$$

where the elements of t are random numbers following a uniform distribution while maintaining Hermiticity. This can be achieved by generating random matrices T_1 and T_2 to construct $T = T_1 + iT_2$, and then symmetrizing as $t = \frac{T+T^\dagger}{2}$. Other types of random t can also be generated to further validate our results. Numerical findings confirm that the overlap matrix approach aligns with exact diagonalization, as shown in Fig. S3.

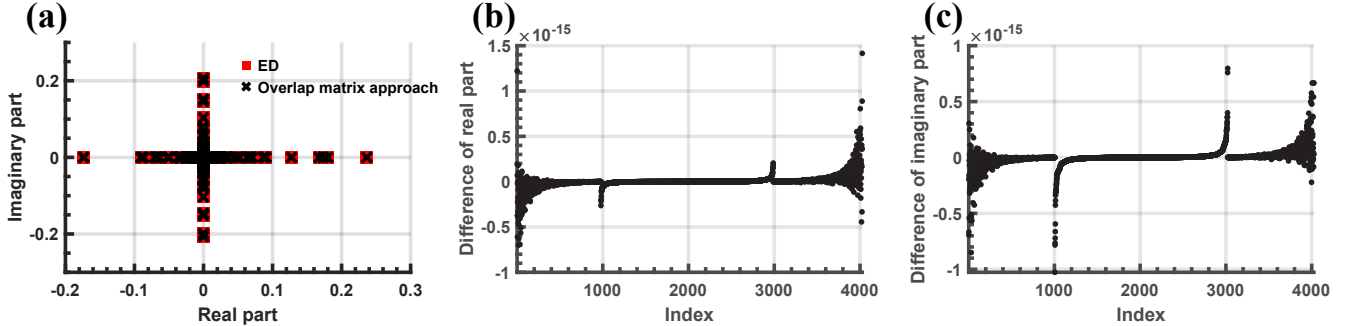


FIG. S3. Comparison of the eigenvalues of $\rho^{T_B^f}$ and $\tilde{\rho}^{T_B^f}$: (a) the congruence of eigenvalues between $\rho^{T_B^f}$ and $\tilde{\rho}^{T_B^f}$; (b) difference in real parts of eigenvalues; (c) difference in imaginary parts of eigenvalues. We select $N = 12$ with an even bipartite geometry. The results indicate that the difference is on the order of 10^{-15} , demonstrating near-perfect agreement.

Appendix D: A proof of rationality of partial trace in the overlap matrix approach

In this appendix, we expand the Eq. (10) into Fock space and compare with the reduced density matrix partially traced in the original basis. We prove that these two equations are completely identical.

We start from the eigenstate

$$\begin{aligned}
|\Psi\rangle &= \prod_{\alpha=1}^M f_{\alpha}^{\dagger}|0\rangle \\
&= \prod_{\alpha=1}^M \sum_{i=1}^N \left(c_i^{\dagger} U_{i,\alpha} \right) |0\rangle \\
&= \sum_{i_1, i_2, \dots, i_M} U_{i_1,1} U_{i_2,2} \cdots U_{i_M,M} c_{i_1}^{\dagger} c_{i_2}^{\dagger} \cdots c_{i_M}^{\dagger} |0\rangle \\
&= \sum_{1 \leq j_1 < j_2 < \dots < j_M \leq N} \left(\sum_{\sigma \in S_M} \text{sgn}(\sigma) U_{j_{\sigma(1)},1} U_{j_{\sigma(2)},2} \cdots U_{j_{\sigma(M)},M} \right) c_{j_1}^{\dagger} c_{j_2}^{\dagger} \cdots c_{j_M}^{\dagger} |0\rangle \\
&= \sum_{1 \leq j_1 < j_2 < \dots < j_M \leq N} \det \begin{pmatrix} U_{j_1,1} & U_{j_1,2} & \cdots & U_{j_1,M} \\ U_{j_2,1} & U_{j_2,2} & \cdots & U_{j_2,M} \\ \vdots & \vdots & \ddots & \vdots \\ U_{j_M,1} & U_{j_M,2} & \cdots & U_{j_M,M} \end{pmatrix} c_{j_1}^{\dagger} c_{j_2}^{\dagger} \cdots c_{j_M}^{\dagger} |0\rangle \\
&\equiv \sum_J \det(U_J) |J\rangle,
\end{aligned} \tag{D1}$$

where in the fourth line $\sum_{\sigma \in S_M}$ represents the summation over all elements of the M th-order symmetric group S_M (M denotes the particle number) and in the last line J implies a permitted sequence of $\{j_1, j_2, \dots, j_M\}$. Accordingly the density matrix

$$\begin{aligned}
\rho &= \sum_{J,K} \det(U_J) \det(U_K^*) |J\rangle \langle K| \\
&= \sum_{J,K} \det(U_J) \det(U_K^*) |J_A, J_B\rangle \langle K_A, K_B|.
\end{aligned} \tag{D2}$$

The partial trace operation ensures that the particles in region B remain the same in both bra and ket states, i.e. $J_B = K_B$. Then we decompose the numerous terms in ρ_A based on the particles in region A

$$\rho_A = \sum_{m=0}^{\min(M, |A|)} \sum_{\substack{J_A, K_A \subseteq A \\ |J_A|=|K_A|=m}} \left(\sum_{\substack{J_B \subseteq B \\ |J_B|=M-m}} \det(U_{J_A \cup J_B}) \det(U_{K_A \cup J_B})^* \right) |J_A\rangle \langle K_A|. \tag{D3}$$

It should be noted that the maximum particle number in region A is $\min(M, |A|)$, where $|A|$ represents the the number of sites in region A . From Sec. II we also know that rotating $\{f_{\alpha}\}_{\alpha=1}^M$ to $\{d_{Ai}\}_{i=1}^M$ and $\{d_{Bi}\}_{i=1}^M$ does not alter the density matrix. Hence the reduced density matrix can also be expressed as

$$\rho_A = \sum_{m=0}^{\min(M, |A|)} \sum_{\substack{J_A, K_A \subseteq A \\ |J_A|=|K_A|=m}} \left(\sum_{\substack{J_B \subseteq B \\ |J_B|=M-m}} \det((U\mathcal{U})_{J_A \cup J_B}) \det((U\mathcal{U})_{K_A \cup J_B})^* \right) |J_A\rangle \langle K_A|. \tag{D4}$$

Then we expand the Eq. (10):

$$\begin{aligned}
\tilde{\rho}_A &= \text{Tr}_B \tilde{\rho} \\
&= \prod_{\gamma=1}^M (P_{\gamma} |1_{A_{\gamma}}\rangle \langle 1_{A_{\gamma}}| + (1 - P_{\gamma}) |0_{A_{\gamma}}\rangle \langle 0_{A_{\gamma}}|) \\
&= \prod_{\gamma=1}^M \left(P_{\gamma} \frac{\sum_{\alpha=1}^M \sum_{j \in A} c_j^{\dagger} U_{j,\alpha} \mathcal{U}_{\alpha,\gamma} |0\rangle \langle 0| \sum_{\beta=1}^M \sum_{j \in A} c_j U_{j,\beta}^* \mathcal{U}_{\beta,\gamma}^*}{\sqrt{P_{\gamma}}} + (1 - P_{\gamma}) |0\rangle \langle 0| \right) \\
&= \prod_{\gamma=1}^M \left(\sum_{\alpha=1}^M \sum_{j \in A} c_j^{\dagger} U_{j,\alpha} \mathcal{U}_{\alpha,\gamma} |0\rangle \langle 0| \sum_{\beta=1}^M \sum_{k \in A} c_k U_{k,\beta}^* \mathcal{U}_{\beta,\gamma}^* + \sum_{\alpha=1}^M \sum_{j \in B} U_{j,\alpha} \mathcal{U}_{\alpha,\gamma} |0\rangle \langle 0| \sum_{\beta=1}^M U_{j,\beta}^* \mathcal{U}_{\beta,\gamma}^* \right),
\end{aligned} \tag{D5}$$

where the symbol $\tilde{\rho}_A$ is introduced to distinguish it from the original reduced density matrix. In the fourth line we express $1 - P_\gamma$ as $\sum_{j \in B} \sum_{\alpha, \beta=1}^M U_{j,\alpha} \mathcal{U}_{\alpha,\gamma} U_{j,\beta}^* \mathcal{U}_{\beta,\gamma}^*$, which can be verified by the identity $(\mathcal{U}^\dagger M_B \mathcal{U})_{\alpha\beta} = \delta_{\alpha\beta} (1 - P_\alpha)$. With the essential identity

$$\begin{aligned} 0 &= \sum_{\mu\nu} \sum_{i \in B} \mathcal{U}_{\mu,\beta}^* U_{i\mu}^* U_{i\nu} \mathcal{U}_{\nu\alpha} \\ &= \sum_{i \in B} (\mathcal{U}\mathcal{U})_{i\alpha} (\mathcal{U}\mathcal{U})_{i\beta}^*, \end{aligned} \quad (\text{D6})$$

which help derive the equation below

$$\tilde{\rho}_A = \sum_{m=0}^{\min(M, |A|)} \sum_{\substack{J_A, K_A \subseteq A \\ |J_A|=|K_A|=m}} \left(\sum_{\substack{J_B \subseteq B \\ |J_B|=M-m}} \det((\mathcal{U}\mathcal{U})_{J_A \cup J_B}) \det((\mathcal{U}\mathcal{U})_{K_A \cup J_B})^* \right) |J_A\rangle \langle K_A|, \quad (\text{D7})$$

from the Eq. (D5). It is clear to derive it in reverse order. Ultimately we demonstrate that $\rho_A = \tilde{\rho}_A$.

Appendix E: The upper bound of logarithmic negativity in bPT

In this appendix, we derive the upper bound formula for logarithmic negativity, as given in Eq. (27). Based on Ref. [39], the upper bound of logarithmic negativity in bPT is

$$\mathcal{E}(\rho^{T_B^b}) \leq \ln \tilde{\det} \left[\left(\frac{1 + \gamma_\times}{2} \right)^{1/2} + \left(\frac{1 - \gamma_\times}{2} \right)^{1/2} \right] + \ln \tilde{\det} \frac{1 - \gamma^2}{2} + \ln \sqrt{2}, \quad (\text{E1})$$

where the symbol $\tilde{\det}$ indicates that double degenerate eigenvalues of the corresponding matrix are counted only once. A normalized Gaussian density operator is defined as $\rho_\times = \frac{O_+ O_-}{\text{tr}(O_+ O_-)}$. For Gaussian operators

$$\frac{1}{Z_\sigma} \exp \left(\sum_{k,l} (W_\sigma)_{k,l} m_k m_l / 4 \right), \quad (\text{E2})$$

the covariance matrix

$$\gamma_\sigma = \tanh \frac{W_\sigma}{2}, \quad \exp(W_\sigma) = \frac{1 + \gamma_\sigma}{1 - \gamma_\sigma}. \quad (\text{E3})$$

As far as the spectrum of ρ_\times is concerned, it can undergo a similarity transformation

$$\gamma_\times \simeq (\mathbb{1} - \gamma_+ \gamma_-)^{-1} (\gamma_+ + \gamma_-). \quad (\text{E4})$$

For particle-conserved free fermions, we can replace γ with the Green function $G_{i,j} = \langle c_i c_j^\dagger \rangle$ and γ_σ with G_σ , and demonstrate that the first two terms of Eq. (E1) precisely correspond to the logarithmic negativity in uPT [1, 37–39].